TISSUE ENGINEERING

Tissue engineering toward temporomandibular joint disc regeneration

Natalia Vapniarsky[1]*, Le W. Huwe[2]*, Boaz Arzi[3], Meghan K. Houghton[4], Mark E. Wong[5], James W. Wilson[5], David C. Hatcher[6], Jerry C. Hu[7], Kyriacos A. Athanasiou[7]†

Treatments for temporomandibular joint (TMJ) disc thinning and perforation, conditions prevalent in TMJ pathologies, are palliative but not reparative. To address this, scaffold-free tissue-engineered implants were created using allogeneic, passaged costal chondrocytes. A combination of compressive and bioactive stimulation regimens produced implants with mechanical properties akin to those of the native disc. Efficacy in repairing disc thinning was examined in minipigs. Compared to empty controls, treatment with tissue-engineered implants restored disc integrity by inducing 4.4 times more complete defect closure, formed 3.4-fold stiffer repair tissue, and promoted 3.2-fold stiffer intralaminar fusion. The osteoarthritis score (indicative of degenerative changes) of the untreated group was 3.0-fold of the implant-treated group. This tissue engineering strategy paves the way for developing tissue-engineered implants as clinical treatments for TMJ disc thinning.

INTRODUCTION

The temporomandibular joint (TMJ), or jaw joint, is a synovial articulation essential for daily functions such as talking and chewing. TMJ dysfunction causes pain and disability in 20 to 25% of adults worldwide (*1*). Not all TMJ disorders require medical intervention, but the associated medical costs and loss of economic productivity are estimated to be $4 billion per year (*2*). The TMJ disc is a fibrocartilaginous structure within the joint that facilitates load bearing, congruity, and smooth movement between the mandibular condyle and skull base. Discal pathology is an antecedent to a series of degenerative changes that can engulf the entire TMJ. Conditions include internal derangement (disc displacement), disc thinning, and perforation (*3*, *4*). Unlike appendicular joints, the early stages of TMJ pathologies (such as disc thinning) are underserved by clinical options. Thus, successful treatment of early TMJ disorders continues to be an unmet goal. Furthermore, the complex and unique anatomy of this joint presents challenges to the development of new surgical strategies for the TMJ, regardless of disease severity.

Clinical options for treating internal derangement vary based on the severity of disc and joint degeneration. Noninvasive and minimally invasive options are used to treat patients in early stages of disease (*5*). More aggressive treatments, such as complete disc removal (*6*–*13*) or prosthetic total joint replacements, are reserved as options of last resort in advanced cases of internal derangement, refractory to other forms of TMJ surgery. However, discectomy appears to result in the development of condylar remodeling, despite an improvement in the patient's symptomatology (*14*–*16*). Minimally invasive treatments do not repair damaged discs, and disc replacement options are lacking. Historical trials with synthetic substitutes, such as the Teflon-Proplast implant, produced catastrophic outcomes (*17*, *18*). There is, to this day, an unmet need for treatments to repair damaged discs to arrest further development toward severe degeneration.

Tissue engineering may offer promising strategies for patients suffering from disc degeneration (*19*–*21*), especially during the early stages of degeneration, such as disc thinning or perforation. Discal regeneration is an active field. For example, scaffolds for TMJ discs have been created with three-dimensional (3D) printed polycaprolactone (*22*), decellularized extracellular matrix (ECM), and other polymers (*23*, *24*). Because scaffold use is associated with foreign body response and toxicity due to scaffold degradation (*25*), scaffold-free methods have been developed (*26*), which create biomimetic tissues without exogenous materials (*27*). Using a scaffold-free, self-assembling process, TMJ disc implants with shape, anisotropy, and biomechanical properties similar to native TMJ discs have been successfully engineered (*28*).

A critical limitation in promoting tissue engineering methods is identifying a cell source appropriate for autologous or allogeneic treatments. Recently, costal cartilage (cartilage from the rib) has emerged as an attractive cell source for TMJ disc engineering (*29*, *30*). The relative abundance of cells from this source, combined with improved scaffold-free techniques, yielded implants with a robust ECM and high mechanical integrity (*31*–*33*). Because this tissue engineering approach requires only a small amount of costal cartilage, this cell source is attractive clinically; large quantities of cells can be obtained with minimal morbidity to the patient.

Toward human translation, tissue-engineered TMJ implants need to be evaluated for safety and efficacy in a suitable large-animal model, requiring the identification of an appropriate defect model for disc thinning, and the development of surgical methods to affix implants into the TMJ. Despite the multitude of in vitro tissue engineering studies, the lack of an appropriate animal model has been a roadblock in the development of new therapies. Comparison of human TMJ disc to multiple species for morphological, biochemical, and biomechanical properties identified the pig model (*34*)—specifically, the Yucatan minipig (*35*)—as suitable for translational studies (*35*). However, a suitable experimental disc defect model to mimic early TMJ disorders, such as TMJ disc thinning and degeneration, did not exist.

Here, we report a series of studies culminating in the examination of allogeneic tissue-engineered implants' safety and reparative capacity in a minipig model, compared to empty defect controls (untreated group).

[1]Department of Pathology, Microbiology, and Immunology, University of California, Davis, Davis, CA 95616, USA. [2]Department of Biomedical Engineering, University of California, Davis, Davis, CA 95616, USA. [3]Department of Surgical and Radiological Sciences, School of Veterinary Medicine, University of California, Davis, Davis, CA 95616, USA. [4]Directorate for Computer and Information Science and Engineering, National Science Foundation, Alexandria, VA 22314, USA. [5]Department of Oral and Maxillofacial Surgery, University of Texas School of Dentistry, Houston, TX 77054, USA. [6]Diagnostic Digital Imaging Center, Sacramento, CA 95825, USA. [7]Department of Biomedical Engineering, University of California, Irvine, Irvine, CA 92697, USA.
*These authors contributed equally to this work as co-first authors.
†Corresponding author. Email: athens@uci.edu

We established a surgical approach and implant fixation method to test the tissue-engineered TMJ disc biomimetic implants, engineered from allogeneic costal chondrocytes, in the orthotopic environment of the TMJ using a clinically relevant early-stage TMJ disc disease model. Our studies evaluated the hypothesis that a tissue-engineered implant would provide sufficient function to promote healing in a defect modeling TMJ disc thinning.

RESULTS

TMJ implants, engineered from expanded costal chondrocytes, are mechanically robust

Tissue-engineered implants were formed using allogeneic costal chondrocytes in conjunction with a scaffold-free, self-assembling process (Fig. 1A) (*26*, *31*). Costal chondrocytes were passaged twice (expansion factor of 64), using a previously optimized protocol (*32*), while retaining the chondrocytic phenotype using an aggregate redifferentiation method (*31*). Implant properties were enhanced by treating self-assembled constructs with bioactive and mechanical stimuli consisting of transforming growth factor–β1 (TGF-β1), chondroitinase ABC, lysyl oxidase–like 2, and passive axial compression. This combination of stimuli was optimized in previous studies for self-assembled cartilage implants (*36*), resulting in an enhancement of collagen production, matrix compaction (*36*), and collagen cross-linking (*37*, *38*). Tissue-engineered implants were 8 mm × 8 mm × 0.4 mm (Fig. 1B), exhibiting robust matrix in the absence of scaffolds (Fig. 1C).

To ensure that the implants were suitable for in vivo load bearing, implant quality was assessed using histology, mechanical testing, and biochemical testing. The cells in the implants were viable and homogeneously distributed (Fig. 1C). Glycosaminoglycan (GAG) and collagen per wet weight were 4.1 and 2.4%, respectively (table S1, tabs 1 and 2). Instantaneous compressive and relaxation modulus values at 20% strain measured 370 and 47 kPa, respectively (table S1, tabs 3 and 4). Tensile Young's modulus and ultimate tensile strength (UTS) were 2.9 and 1.1 MPa, respectively (fig. S1 and table S1, tabs 5 and 6). The mechanical values were noted to approach those of native minipig TMJ discs. The degree of biomimicry to native TMJ disc properties and the tissue-engineered implants' suitability for in vivo implantation were evaluated using a modified functionality index (FI) (*28*), which compared the implants' mechanical and biochemical properties to those of native Yucatan minipig TMJ discs (*35*). The FI (see Supplementary Materials and Methods, "Fabrication of tissue engineered implants" section, eq. S1) normalizes implant properties to native TMJ disc properties, and an FI of 1 represents 100% of native tissue properties. The average implant FI was 0.42 or 42% of the native TMJ disc's cumulative biochemical and biomechanical properties. Given previous small-animal in vivo data demonstrating the improvement of tissue-engineered construct properties after implantation (*39*), the tissue-engineered implants were considered suitable for further assessment in vivo in a minipig model.

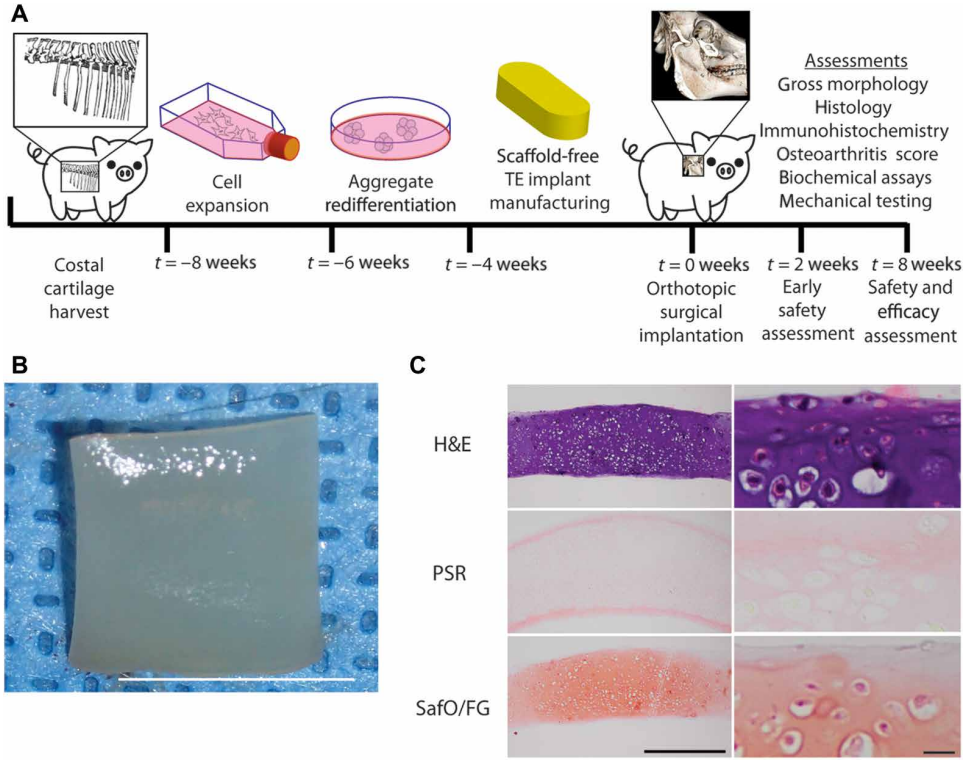

Fig. 1. Formation of tissue-engineered implants from costal chondrocytes and representative gross morphological and histological images. (**A**) Diagram depicting the tissue engineering strategy and timeline from isolation of costal chondrocytes to the implants' in vivo assessment. Costal cartilage from minipigs was harvested as an allogeneic donor chondrocyte source. The chondrocytes were then expanded in monolayer, redifferentiated in an aggregate culture, and self-assembled into 3D constructs using a scaffold-free approach. Upon construct maturation, the tissue-engineered (TE) implants' safety and efficacy were assessed via orthotopic implantation into TMJ discs. (**B**) Tissue-engineered implants' gross morphology. The tissue-engineered implants' dimensions shown are 8 mm × 8 mm × 0.4 mm and trimmed before implantation (scale bar, 5 mm; $n = 24$). (**C**) Tissue-engineered implants' histology at time of implantation. Shown are hematoxylin and eosin (H&E)–, PicroSirius Red (PSR)–, and Safranin O/fast green (SafO/FG)–stained sections (scale bars, 500 and 20 μm, respectively; $n = 12$).

The intralaminar fenestration surgical technique reliably recreates disc thinning to allow for orthotopic implantation

A suitable defect model and implant fixation method were required to evaluate the tissue-engineered implants' relevance for therapeutic use in TMJ defects. In a preliminary study, a circular defect mimicking human TMJ disc perforation in the minipig disc's posterolateral portion was created and reconstructed with tissue-engineered implants sutured to the surrounding native TMJ disc (fig. S2, A to C). Eight weeks after implantation, it became apparent that the fixation method was inadequate: The implants were dislodged, and the defect remained empty (fig. S2, D to F). Degenerative changes were noted on the opposing condylar surface (fig. S2, G to I). This observation is consistent with other animal studies where disc perforation was used as a surgical technique to create TMJ degeneration (*40*, *41*). From this initial minipig study, we concluded

that direct suturing of implants to a disc perforation defect was ineffective, inducing degenerative changes in the joint.

To overcome these issues, another surgical technique was developed. In this second approach, a horizontal pouch was dissected within the disc's lateral region. After separating the two laminae, a circular fenestration removed disc tissue from the inferior lamina, mimicking human disc thinning (Fig. 2, A to J and A′ to J′). In short, two defects were created: the pouch and the fenestration. To repair these defects, a tissue-engineered implant was placed in the pouch to cover the fenestration, and the pouch's margins were sutured to retain the implant in position. This method eliminated the need to have suture knots facing the articulating surfaces to retain the implant. Gross (Fig. 3, A and B) and histological examination 2 and 8 weeks after implantation in vivo showed that this intralaminar technique was effective in securing the implant to the native tissue (Fig. 3, C and D). The histological data suggest that the technique was sufficient to model the ability of a tissue-engineered implant to heal a dissected pouch in the disc and also to repair disc thinning (the fenestration).

Tissue-engineered implants are durable after implantation

The tissue-engineered implants were evaluated at 2 and 8 weeks after implantation. With the intralaminar fenestration technique, the implants remained in place and did not dislodge. The implants retained their shape and size (Fig. 3, E to H), were partially fused with the surrounding native tissue at 2 weeks, and were completely fused at 8 weeks. There was no evidence of implant breakage or fragmentation. These observations, collectively, indicated that the implants were sufficiently robust to withstand forces in the orthotopic environment. They also confirmed the effectiveness of our fixation method.

The tissue-engineered implants excised from the TMJs were mechanically tested for tensile stiffness and strength at 8 weeks after implantation. The results demonstrated that the Young's modulus of tissue-engineered implants 8 weeks after implantation was similar to that at the time of implantation (fig. S1). This suggests that the implants' integrity did not deteriorate in vivo in a biomechanically loaded environment and compared favorably with the in vitro controls, which also maintained their compressive and tensile properties over 5 weeks in culture (fig. S1).

Allogeneic tissue-engineered implants are safe and tolerated immunologically

Within 10 days after surgery, all external incisions healed completely. At 8 weeks after surgery, minimal skin scarring was present (fig. S3). All animals progressed through the study uneventfully, maintained weight, and did not experience issues with chewing or retrieving food. One animal developed unilateral septic arthritis in the treated joint that was considered iatrogenic in origin. Throughout the study, there was no evidence of leukocytosis or abnormal values on routine blood work (table S1, tab 7). Upon sacrifice and postmortem examination, there was no evidence of inflammation or neoplastic growth in the implanted joints. In all animals, treated or with empty controls, the joint capsules were completely intact with minimal joint fluid; the synovial lining displayed none or minimal hyperplasia. Full-body necropsy examined the histomorphology in multiple organ systems including integument, cardiovascular, respiratory, musculoskeletal, digestive, urogenital, endocrine, and nervous systems. All systems were within normal limits and exhibited no evidence of cellular damage, inflammation, or neoplastic growth. The mandibular and retropharyngeal lymph nodes' size, shape, and consistency were also within normal limits in both groups. Collectively, these findings indicated no evidence of adverse systemic response to allogeneic implants.

Histological (Fig. 3, C to H) and immunohistochemical (Fig. 3, I to N) evaluations of treated TMJ discs revealed minimal to mild lymphocytic inflammation around the implants. Semiquantitative immunohistochemical assessment for CD3 (T cell) and CD20 (B cell) immunoreactivity detected moderate numbers of both cell types, and the number of lymphocytes did not change markedly from 2 to 8 weeks after implantation (Fig. 3, I to L). CD68 (macrophage) immunoreactivity was rare to nonexistent around or within the implants (Fig. 3, M and N). Furthermore, there was no histological evidence of multinucleated giant cells, polymorphonuclear cells (neutrophils and eosinophils), or capsule formation around the implants, indicating that the implants were tolerated immunologically and did not provoke a foreign body response.

Tissue-engineered implants prevent gross, degenerative changes to the condylar head caused by disc thinning

Gross and histological examinations of condylar surfaces were informative in determining the effectiveness of tissue-engineered implant treatment in delaying or preventing degeneration of the joint's articulating components (mandibular head and temporal articular fossa). Mandibular condyles were scored according to International Cartilage Repair Society guidelines (*42*), where a lower score indicates less degeneration. The mandibular head surfaces in groups that received tissue-engineered implants were normal (Fig. 4, A to C) or showed minor abnormalities, such as focal surface erosions and occasional small osteophytes (fig. S4, A to F). Mandibular condyles from empty defect control groups displayed more extensive surface irregularities, deep cavitations, subchondral cysts, large osteophytes, and condylar bone flattening and deformation (Fig. 4, D to F, and fig. S4, G to L). Corresponding histological analysis showed normal articular surfaces in the treated group (fig. S5, A to F) and multiple surface irregularities in the untreated group (fig. S5, G to L). These observations are consistent with previous work linking degenerative changes to discal pathologies (*40*, *41*, *43*–*47*).

Tissue-engineered implants improve the stiffness and closure of TMJ disc defects

The efficacy of healing was determined by the functional assessment of repair tissue and extent of closure of the pouch and fenestration defects. Visual and histological assessments showed that fenestrations overlaid with implants underwent defect closure and healing more completely than untreated TMJ discs (Fig. 4, G to N). In all six treated TMJ discs, new repair tissue formed in the site of fenestration, closing the defect (Fig. 4, G to J). In the control group, three discs exhibited the fenestrations' partial closure with repair tissue, whereas the other three discs lacked new tissue formation resulting in open fenestrations (Fig. 4, K to N). The extent of healing was quantified by measuring the perimeter of closure of the pouch and fenestration using histological sections (table S1, tab 8). Upon examination of the implant-treated group versus untreated discs (Fig. 5A), 90% closure of the perimeter of the pouch and fenestration defects was achieved (Fig. 5B). In the untreated TMJ discs, only 20% of the defect perimeters were closed (Fig. 5B). The significant difference ($P < 0.05$) between the groups indicates that the tissue-engineered implants facilitated the repair of disc thinning.

The stiffness of the repair tissue that filled the fenestration defects in the discs was mechanically tested under tension. Treatment with

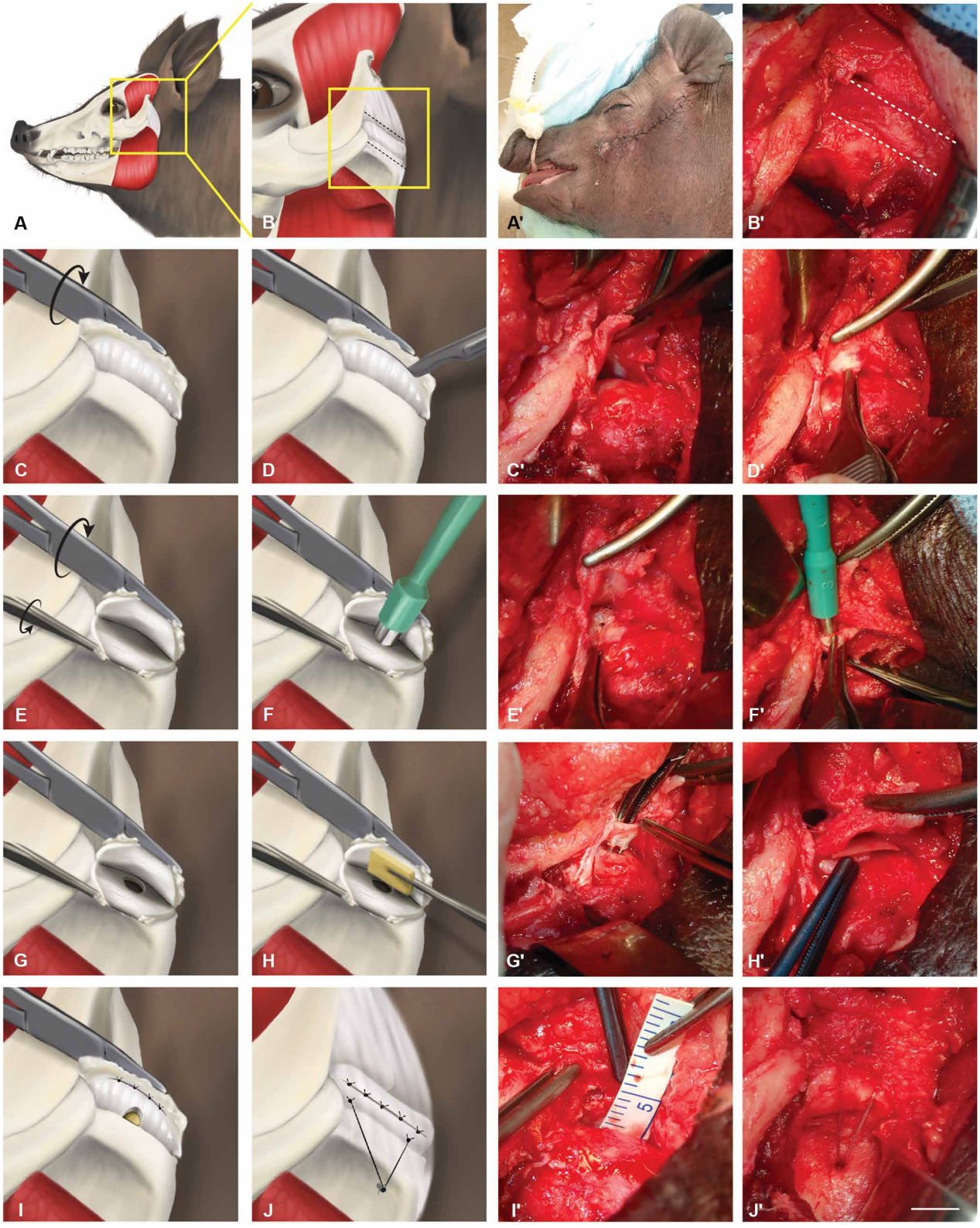

Fig. 2. Schematic and intraoperative images demonstrating the intralaminar fenestration surgical technique. This technique allowed modeling of TMJ disc thinning, orthotopic implantation, and the tissue-engineered implant's fixation in the TMJ disc of a minipig. (**A**, **A**′, **B**, and **B**′) Posterolateral surgical approach to the TMJ disc is demonstrated. (**C** and **C**′) The disc is partially released from its posterolateral attachments, gently pulled caudally, and rotated superiorly. (**D**, **D**′, **E**, and **E**′) Horizontal dissection is performed to create a bilaminar pouch. (**F**, **F**′, **G**, and **G**′) A 3-mm fenestration defect is made in the pouch's inferior lamina. (**H** and **H**′) The tissue-engineered implant is inserted into the pouch. (**I**, **I**′, **J**, and **J**′) The pouch is closed with sutures, and the disc attachments are reproduced with Quickanchor Plus and #0 suture. Scale bar, 5 mm.

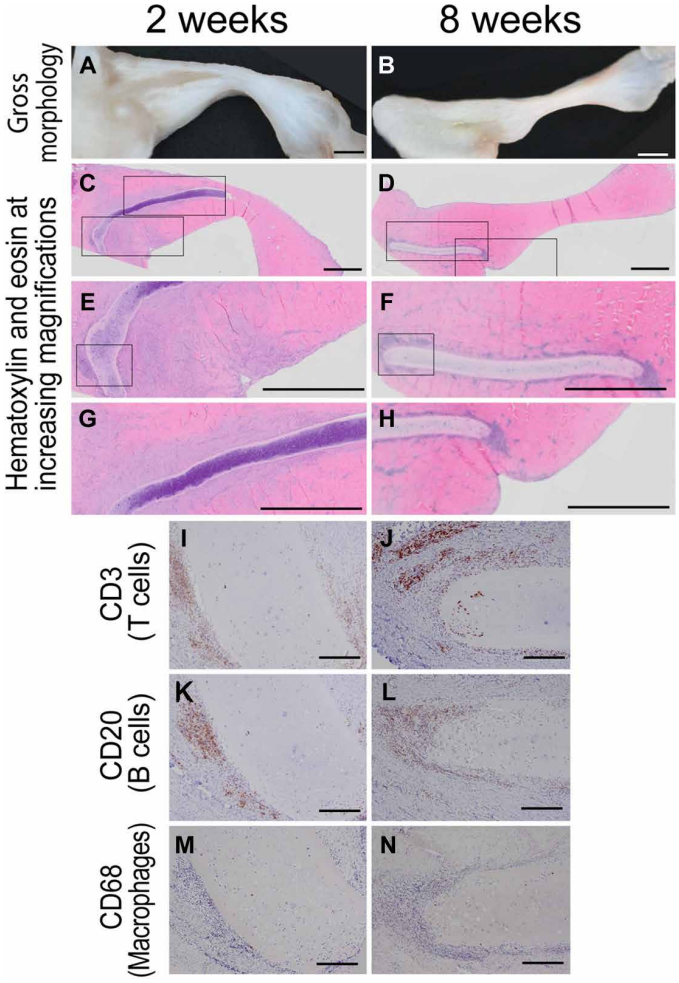

Fig. 3. Histological and immunohistochemical assessment of integration and safety of the tissue-engineered implants. (**A** and **B**) Gross morphology of the sections obtained from the minipig discs treated with tissue-engineered implants, 2 and 8 weeks after implantation, respectively. (**C** and **D**) Low-magnification H&E histology of the disc section containing a tissue-engineered implant, which appears as a purple band at 2 weeks and as a pale pink band at 8 weeks, respectively. (**E** to **H**) Higher magnification of the H&E sections containing implants at 2 and 8 weeks after implantation, respectively. (**I** and **J**) Immunoreactivity for T cells (CD3) at 2 and 8 weeks, respectively. (**K** and **L**) Immunoreactivity for B cells (CD20) at 2 and 8 weeks, respectively. (**M** and **N**) Immunoreactivity for macrophages (CD68) at 2 and 8 weeks, respectively. Scale bars, 2 mm (A to H) and 200 μm (I to N).

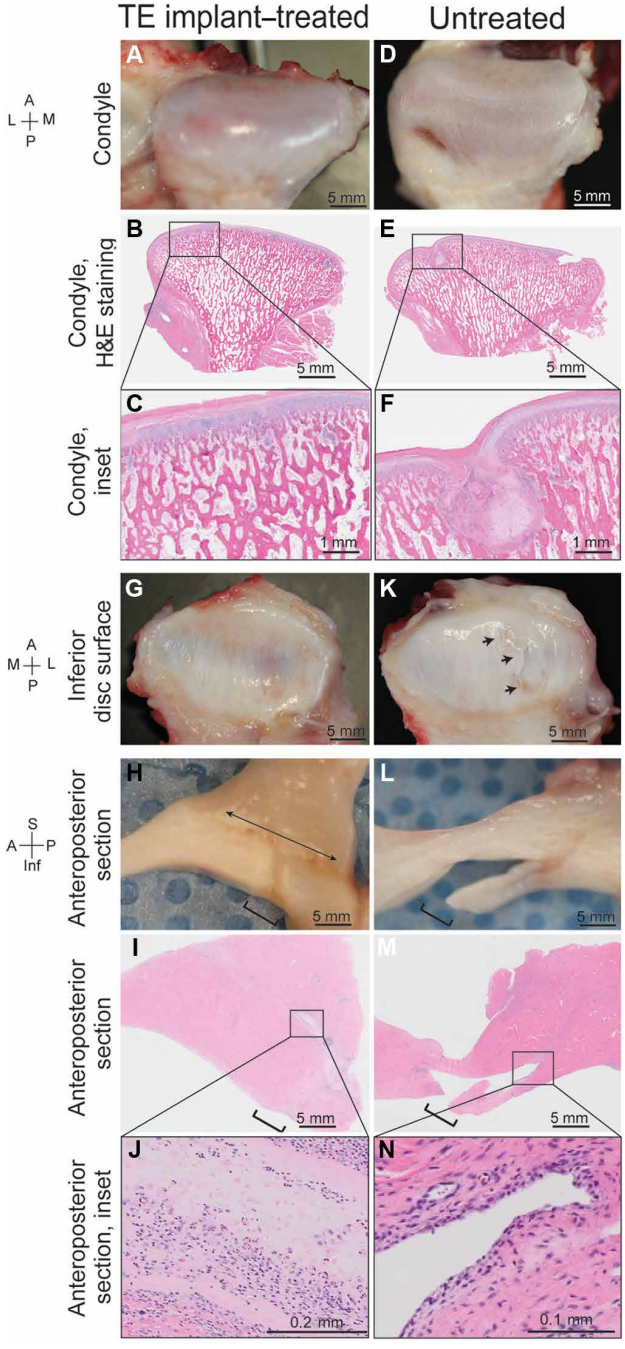

Fig. 4. Gross morphological and histological assessments of the TMJ disc and mandibular heads comparing the tissue-engineered implant–treated group to the untreated group at 8 weeks after implantation ($n = 6$). A, anterior; P, posterior; L, lateral; M, medial; S, superior; Inf, inferior. (**A** to **F**) Gross morphology and histology of the mandibular head articular surfaces in the treated versus untreated cases. (**G**) Gross morphology of the inferior surface of treated TMJ discs. (**H**) Gross morphology of sagittal (anteroposterior) sections of implant-treated discs. The arrow marks the implant's location and orientation. The square bracket indicates the location of the healed defect. (**I** and **J**) Low- and high-magnification H&E histology images of implant-treated discs. The square bracket indicates the healed defect (I). (**K**) Gross morphology of the inferior surface of untreated TMJ discs. (**L**) Gross morphology of sagittal (anteroposterior) sections of untreated discs. The square bracket indicates the open defect's location. (**M** and **N**) Low- and high-magnification H&E histology images of untreated discs. The square bracket indicates the open defect (M).

the tissue-engineered implants resulted in the formation of repair tissue with a Young's modulus that was 3.4-fold greater than the repair tissue in untreated TMJ discs (Fig. 5C and table S1, tab 9). In addition, it was found that the tensile stiffness of the repair tissue that sealed the defects in the treated defects was 37.4% of the native tissue value (*35*) in this region. In contrast, the repair tissue in the untreated discs approached 10.9% of native tissue tensile stiffness (*35*). A similar trend was observed for the repair tissue's UTS in treated discs versus untreated discs (table S1, tab 10), where the repair tissue's UTS reached 23.3 and 8.9% of native values (*35*), respectively. A more robust quality of tissue repair was achieved with the tissue-engineered implant.

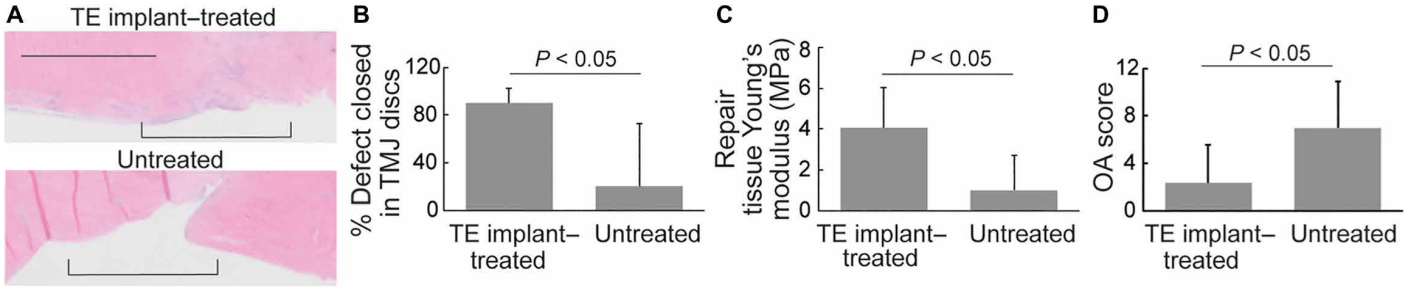

Fig. 5. Quantitative assessment of the efficacy of the tissue-engineered implant to heal the TMJ disc defect. (**A**) Histological appearance of a defect treated with tissue-engineered implant versus untreated discs. Square brackets indicate the defect location. Scale bar, 2 mm. (**B**) Percent of the combined pouch and fenestration defect perimeter closure indicative of the extent of healing. (**C**) Young's modulus values representing the tensile stiffness of the repair tissue that formed in the discs treated with tissue-engineered implant versus untreated discs. (**D**) Osteoarthritis (OA) scores derived from evaluation of the mandibular heads in implant-treated groups versus untreated groups to measure TMJ degeneration. For all graphs, bars indicate means ± SD ($P < 0.05$). Student's t test was used with $n = 6$, and all data were taken at 8 weeks after implantation.

Tissue-engineered implants improve osteoarthritis scores

Degeneration of untreated joints, as measured using the osteoarthritis score, was 7.0 ± 3.9 (Fig. 5D and table S1, tab 11), whereas that of the implant-treated group was 2.3 ± 3.2. Thus, the total osteoarthritis score in the treated group was one-third ($P < 0.05$) of the untreated controls. These data suggest that (i) the intralaminar fenestration technique created a defect, akin to disc thinning, that mimicked disease by promoting 3.0-fold higher degenerative changes in the condylar articular surface, and (ii) implantation of the tissue-engineered construct reduced degeneration, resulting in improved preservation of the articular surfaces.

Tissue-engineered implants adaptively remodel and improve integration stiffness

The intralaminar fenestration technique made a horizontal incision into the TMJ disc, creating two laminae and a pouch in which the implant was inserted. Eight weeks after implantation, defects treated with tissue-engineered implants showed greater integration (fusion) ($P < 0.05$) between the two disc laminae (Fig. 6A). This fusion was observed grossly, confirmed histologically, and quantified mechanically (table S1, tab 12). Untreated discs failed to fuse or achieved limited fusion (Fig. 6B, arrowheads). In the implanted specimens, the interface between the implant and native tissue grossly appeared seamless without voids or gaps (Fig. 6C, arrowheads). To quantify the degree of integration to the native disc, tensile stiffness testing at the interface was performed (Fig. 6A and fig. S6). The stiffness of integration between the two laminae was significantly higher ($P < 0.05$, 3.2-fold) when treated with the tissue-engineered implant than without treatment. Histology confirmed the gross observations and mechanical testing, demonstrating the implants' fusion to the native tissue. Fibroblasts gradually incorporated into the tissue-engineered implant (Fig. 4, I and J). Fusion of native tissue to implant and multifocal ingress into the implant by fibroblast-like cells, presumably derived from the native perivascular environment, were indicative of integration. Histological examination demonstrated that integration progressed from the disc's periphery to central portions (Fig. 3, C to H).

At the time of implantation, the implant appeared to contain more GAG (Fig. 6D) and less collagen (Fig. 6E) than reference values of native tissue biochemical properties (*35*). After implantation, tissue-engineered constructs underwent adaptive remodeling, and biochemical properties approached native tissue values. The implant's GAG content decreased from 4.1 to 0.1 percent per wet weight (%/WW) (Fig. 6D), as evidenced by histological staining (Fig. 6, F to H). Collagen content increased from 2.4 to 8.9%/WW from the time of implantation to 8 weeks after implantation (Fig. 6E); this was also supported by histochemical examinations, which showed a gradual transition from GAG-rich and collagen-poor ECM toward collagen-rich and GAG-poor ECM (Fig. 6, F to K). The initial GAG content in the tissue-engineered implants exceeded that of native tissue (0.8%/WW), and the initial collagen content was lower than the native tissue value (25.0%/WW). A gradual reduction in cellularity was observed histologically, represented by the multifocal eosinophilia (interpreted as cell death) of occasional chondrocytes at 2 weeks after implantation (Fig. 3, C, E, and G), followed by widespread eosinophilia of the cells in the implant lacunae at 8 weeks (Fig. 4J). Cumulatively, histological, biochemical, and mechanical results suggested that the tissue-engineered implant underwent progressive adaptive remodeling to amalgamate with the native tissue.

DISCUSSION

This work demonstrates that tissue-engineered implants produced from allogeneic, passaged costal chondrocytes can be applied to treat TMJ disc thinning, a condition seen in early TMJ disorders that precedes severe degenerative changes in this joint. Using an innovative surgical approach, reproducible defects modeling early-stage TMJ disc disease were treated with tissue-engineered implants. Healing was more robust in the implant-treated discs compared with untreated defects, demonstrating repair of a fenestration defect modeling TMJ disc thinning. Repair tissue formed in response to treatment exhibited a greater Young's modulus than that of the repair tissue formed in untreated discs. The implants also improved closure of the pouch and fenestration defects, and promoted integration with the intralaminar pouch (greater fusion between the implant and surrounding native tissue).

By restoring the mechanical properties of discs that had been subjected to experimental disc thinning, the tissue-engineered implants were associated with a reduction in the articulating surfaces' degeneration while demonstrating continued adaptive remodeling. The allogeneic implants were associated with a minimal immune response and no evidence of acute implant rejection. These results demonstrate a strategy capable of producing healing of TMJ disc thinning, paving the way toward new clinical applications of tissue-engineered solutions for patients with TMJ disc pathologies.

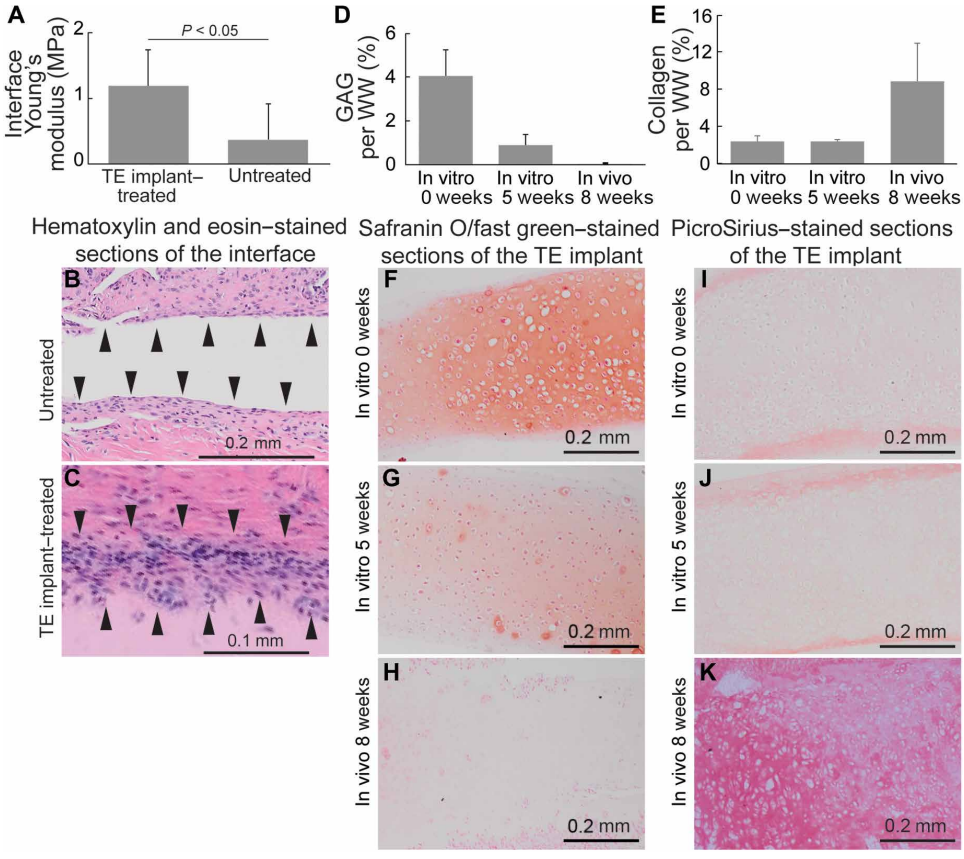

Fig. 6. Integration stiffness at the interface and changes in the biochemical content of the tissue-engineered implants due to adaptive remodeling. (**A**) Young's modulus at the interface of the tissue-engineered implant or untreated defect. Bars indicate means ± SD ($n = 5$ to 6; $P < 0.05$, Student's t test), and all data were taken at 8 weeks after implantation. (**B** and **C**) Representative histology (H&E). Arrowheads show the native-to-native or native-to-implant interface, which is separated by space in the untreated defect. (**D**) GAG content in the tissue-engineered implant at time zero ($n = 6$), after 5 weeks of in vitro culture ($n = 6$), and 8 weeks after implantation ($n = 2$). (**E**) Collagen content in the tissue-engineered implant at time zero ($n = 6$), after 5 weeks of in vitro culture ($n = 6$), and 8 weeks after implantation ($n = 2$). (**F** to **H**) Representative Safranin O/fast green histochemical staining. (**I** to **K**) Representative PicroSirius Red histochemical staining.

A main objective of this study was to use a tissue engineering strategy to address disc thinning before irreversible degenerative changes of the articulating surfaces occur. Current clinical options are limited for patients suffering from disc thinning and degeneration (*5*). Once the disc loses its structure and integrity (*5*), discectomy (disc removal) without replacement is the current standard of care (*48*). Alloplastic disc replacement has been less than satisfactory (*49*, *50*), and the use of autologous fat or dermal grafts has been ineffective in the long term (*51*). This approach attempts to reconstruct damaged discs by repairing and strengthening the existing disc through fibrocartilaginous healing. By preserving joint anatomy, this approach has the potential to reduce degenerative changes at the early stages of injury or pathology, thereby preventing disease progression.

A major advantage of the biomimetic TMJ disc implants developed in this study is that they are completely devoid of exogenous scaffold materials. Exogenous scaffolds, such as poly(lactic acid) and poly(lactic-co-glycolic acid), have been documented to induce a foreign body immune response and capsule formation as well as side effects induced by the by-products of polymer degradation (*52*). The absence of macrophages, foreign body giant cells, and an inflammatory capsule around the implants at 2 and 8 weeks after implantation are indicative of local biocompatibility. A limited lymphocytic response and lack of systemic signs of toxicity and inflammation further reinforce this finding. Ingrowth of fibroblast-like cells into the implants demonstrated the processes of repair, integration, and adaptive remodeling, which appear to be enhanced by a scaffold-free approach to implant fabrication. Following the translational pathway, subsequent studies should track implant versus host cells to determine whether larger implants can similarly be remodeled.

The tissue-engineered implants displayed mechanical properties similar to the native disc, which is crucial for proper function in the mechanically demanding environment of the jaw joint. At the time of implantation, the implant's Young's modulus and the relaxation modulus were similar to the native tissue in the TMJ disc's posterior region, which allowed for immediate load bearing and joint movement upon implantation. The implants also promoted regeneration of the damaged tissue, likely by eliminating stress concentrations that can result from dissimilarity in stiffness between implants and native tissue. The Young's modulus of the repair tissue in the fenestration was greater than repair tissue in the untreated defect, and this was associated with histological evidence of healing. By providing a balanced mechanical environment, the implant treatment protected the condylar surface from degenerative changes, evidenced by a 3.0-fold reduction in the osteoarthritis score. Therefore, the implant's biomechanical mimicry promoted TMJ disc healing.

Integration between cartilaginous tissues and engineered implants has been a clinical challenge for surgeons (*27*). The implants in our study were treated with the cross-linking enzyme lysyl oxidase–like 2. The benefits of using this agent were that (i) it assisted in producing mechanically robust implants, as observed in this study and also shown in previous studies (*19*, *38*), and (ii) it primed tissue-engineered implants to integrate with native tissue (*38*). Both of these benefits promoted success of tissue-engineered implant–based therapy. By improving integration to the surrounding native tissue, the implants closed the surgically created defects with tissue almost indistinguishable from the native disc. Adaptive remodeling of the tissue-engineered implant may also have been facilitated by cell-to-cell communication between chondrocytes in the allogeneic implant and fibrochondrocytes in the native TMJ disc. This tissue engineering strategy solves the persistent problem of cartilage-to-cartilage integration when addressing intracartilaginous defects.

This study's innovative surgical approach examined the tissue-engineered implant's efficacy in an orthotopic environment in a large,

clinically relevant animal model. The dearth of such studies is due in part to the absence of appropriate models of disease and the challenges of implant fixation. Using both cadaveric and live animal studies, the intralaminar fenestration technique was developed to simulate pathology in the clinically relevant posterolateral quadrant of the disc, where disc thinning and perforation are most frequent in humans (*53*). The TMJ disc defect size examined in this study, when normalized to surface area, corresponds proportionally to a 2-cm^2 defect of knee cartilage.

Another advantage of the intralaminar fenestration technique is the ability to secure the engineered implant to native tissues without direct sutures. Suturing tissue-engineered implants to tissue defects is a commonly used fixation method (*54*). However, our early attempts to attach implants to disc defects using sutures resulted in failed cartilage-to-cartilage healing. In addition, suture material at the articular surface created surface irregularities and stress concentrations that disrupted smooth joint articulation. By placing sutures away from the articular surface, the joint's smooth functioning was not impaired, and only minor degenerative changes on the condylar surface in treated joints were observed. The intralaminar fixation technique is, therefore, a promising method that should be considered not only in the TMJ but also in other anatomic locations, such as the knee meniscus, hyaline articular cartilage, and intervertebral disc.

The animal model used in this study opens the door for examination into how tissue-engineered implants perform in the location where implants would likely be used in patients with TMJ internal derangement. For the TMJ, in particular, minipigs serve as an excellent preclinical model because of their similarities to human TMJ discs, with respect to morphology, biochemistry, and biomechanics (*35*). Minipigs also have similar chewing patterns that address an omnivorous diet similar to humans (*55*). The maxillofacial surgeons in this study were successfully able to transfer clinical techniques used in humans to operate in minipigs; we expect the same to be true when techniques developed in minipigs are translated to human patients.

The allogeneic costal chondrocytes used in this study did not provoke an acute immune rejection. The allogeneic approach's success supports the development of off-the-shelf implants. The maintenance of mechanical properties in vitro further strengthens the case for allogeneic products. Because there is limited to no healthy TMJ disc tissue that can be sourced from patients with TMJ disorders, and given that previous work has shown that TMJ disc cells are almost completely inadequate for tissue engineering (*56*–*59*), autologous TMJ cells do not appear to be a viable option. In contrast, as a relatively minimally invasive harvesting procedure, the use of costal chondrocytes could easily be part of autologous therapies. Use of autologous cells may offer additional benefits not observed in this study; however, the disadvantages associated with second-site surgery and delays associated with implant creation also need to be considered. Subsequent studies can also consider the use of cell mixtures, such as costal chondrocytes with fibroblasts or other collagen-producing cells.

A limitation of this study is the lack of a comparative therapy (for example, a synthetic or natural ECM scaffold) and lack of analysis of human TMJ patient samples to directly demonstrate the model's similarity with human disease. In addition, a partial thickness defect only mimics disc thinning in an otherwise nonpathologic joint, which motivates further studies assessing the performance of tissue-engineered implants in an inflamed joint environment. Because disc thinning represents one aspect of TMJ degeneration, additional studies are warranted to examine the performance and efficacy of tissue-engineered implants in treating fully perforated defects as well as larger defects.

This work presents successful healing of TMJ disc defects in a large-animal model. Healing was accomplished in an orthotopic environment using implants, tissue-engineered via a scaffold-free approach using passaged and redifferentiated costal chondrocytes. The intralaminar fenestration technique provided a secure fixation of the implants in a tissue that experiences repetitive mechanical stresses. The implants' mechanical properties at the time of implantation allowed the implants to withstand joint loads and reduce degenerative changes. The quality of the resultant repair tissue, the robustness of integration, the completeness of defect closure, and the absence of an adverse immune response indicate successful TMJ disc regeneration. The presence of inflammatory cells at the site of implantation 8 weeks after surgery, concurrently with enhanced healing, echoes evolving views on the beneficial effects of inflammation on healing (*60*, *61*). Building upon these results, studies may now be performed to assess long-term safety and efficacy. Refinement of the intralaminar fenestration technique may eventually lead to arthroscopic procedures that are less invasive. The tissue-engineered implants could also be deployed in a pathologic environment to determine their effectiveness under inflammatory or adverse loading conditions. Overall, this study advances tissue engineering as an approach for regeneration of TMJ discs to address disc thinning in the pathogenesis of TMJ degeneration.

MATERIALS AND METHODS

Study design

The objectives of this study were (i) to tissue engineer TMJ disc biomimetic implants from allogeneic costal chondrocytes, (ii) to develop a clinically relevant, large-animal TMJ disc disease model, (iii) to establish a surgical approach and implant fixation method in vivo, and (iv) to evaluate the tissue-engineered implants for safety and efficacy in the orthotopic environment of the TMJ. This work was a randomized, nonblinded, controlled laboratory experiment. TMJ disc–specific implants were fabricated using the self-assembling process. An intralaminar fenestration technique was developed in porcine cadavers and then implemented in live animals, mimicking TMJ disc thinning. This technique also allowed the secure fixation of the implant in situ. Finally, the tissue-engineered implants were evaluated for safety and efficacy in the minipig disc thinning TMJ model. The quality, safety, and efficacy of the tissue-engineered implants were assessed grossly, mechanically, biochemically, and histologically. The sample size of $n = 6$ per group for in vitro assessments was based on an SD of 30% (the highest SD observed during preliminary implant tensile moduli testing), power of 80%, difference to detect 50% of the mean average, and α of 0.05. The in vivo assessment was carried out on a total of 19 male minipigs. The sample size of $n = 6$ per group for in vivo experiments was calculated on the basis of an SD of 28% (highest SD observed in TMJ native disc tensile moduli measurements), power of 80%, difference to detect 50% of the mean average, and α of 0.05. Specific information on sample size, data collection, and inclusion and exclusion criteria are provided in the context of each experimental stage. Reagents and methods used for histological analysis are shown in table S1 (tab 13).

Statistical analysis

All data are reported as means ± SD. Wilcoxon/Kruskal-Wallis rank test was performed to compare the tensile properties of the tissue-engineered implants at various time points, using JMP 13 statistical software. All other comparisons in the study were performed using Student's *t* tests.

SUPPLEMENTARY MATERIALS

www.sciencetranslationalmedicine.org/cgi/content/full/10/446/eaaq1802/DC1
Materials and Methods
Fig. S1. Tissue-engineered implants' tensile and compressive properties at various time points in vitro (t = 0 and 5 weeks) and in vivo (t = 8 weeks).
Fig. S2. Method and outcome of the preliminary in vivo experiment exploring disc perforation defect and suture fixation of tissue-engineered implants (n = 3 shown).
Fig. S3. Representative external appearances of implantation sites 8 weeks after surgery in tissue-engineered implant–treated groups and empty controls, respectively (n = 6).
Fig. S4. The mandibular head articulating surfaces' gross appearances in tissue-engineered implant–treated groups and untreated controls 8 weeks after implantation (n = 6).
Fig. S5. Low-magnification histology (H&E) of the mandibular heads of tissue-engineered implant–treated groups and untreated controls 8 weeks after implantation (n = 6).
Fig. S6. Schematic diagram showing specimen preparation for mechanical and histological assessments of the tissue-engineered implant–treated TMJ discs and of the discs with untreated defects.
Fig. S7. The intralaminar fenestration technique's ex vivo feasibility validation (n = 3).
Table S1. Primary data (Excel file).
References (*62*–*65*)

REFERENCES AND NOTES

1. M. K. Murphy, R. F. MacBarb, M. E. Wong, K. A. Athanasiou, Temporomandibular joint disorders: A review of etiology, clinical management, and tissue engineering strategies. *Int. J. Oral Maxillofac. Implants* **28**, e393–e414 (2013).
2. B. A. White, L. A. Williams, J. R. Leben, Health care utilization and cost among health maintenance organization members with temporomandibular disorders. *J. Orofac. Pain* **15**, 158–169 (2001).
3. W. B. Farrar, W. L. McCarty Jr., The TMJ dilemma. *J. Ala. Dent. Assoc.* **63**, 19–26 (1979).
4. C. H. Wilkes, Internal derangements of the temporomandibular joint. Pathological variations. *Arch. Otolaryngol. Head Neck Surg.* **115**, 469–477 (1989).
5. A. Aryaei, N. Vapniarsky, J. C. Hu, K. A. Athanasiou, Recent tissue engineering advances for the treatment of temporomandibular joint disorders. *Curr. Osteoporos. Rep.* **14**, 269–279 (2016).
6. A. B. Holmlund, G. Gynther, S. Axelsson, Diskectomy in treatment of internal derangement of the temporomandibular joint. Follow-up at 1, 3, and 5 years. *Oral. Surg. Oral. Med. Oral Pathol.* **76**, 266–271 (1993).
7. S. J. McKenna, Discectomy for the treatment of internal derangements of the temporomandibular joint. *J. Oral. Maxillofac. Surg.* **59**, 1051–1056 (2001).
8. J. Nyberg, R. Adell, B. Svensson, Temporomandibular joint discectomy for treatment of unilateral internal derangements—A 5 year follow-up evaluation. *Int. J. Oral Maxillofac. Surg.* **33**, 8–12 (2004).
9. L. Eriksson, P.-L. Westesson, Long-term evaluation of meniscectomy of the temporomandibular joint. *J. Oral. Maxillofac. Surg.* **43**, 263–269 (1985).
10. L.-G. Hansson, L. Eriksson, P.-L. Westesson, Magnetic resonance evaluation after temporomandibular joint diskectomy. *Oral Surg. Oral Med. Oral Pathol.* **74**, 801–810 (1992).
11. C. M. Silver, Long-term results of meniscectomy of the temporomandibular joint. *Cranio* **3**, 46–57 (1984).
12. S. Takaku, T. Toyoda, Long-term evaluation of discectomy of the temporomandibular joint. *J. Oral. Maxillofac. Surg.* **52**, 722–726; discussion 727–728 (1994).
13. M. Tolvanen, V. J. Oikarinen, J. Wolf, A 30-year follow-up study of temporomandibular joint meniscectomies: A report on five patients. *Br. J. Oral Maxillofac. Surg.* **26**, 311–316 (1988).
14. G. Agerberg, M. Lundberg, Changes in the temporomandibular joint after surgical treatment. A radiologic follow-up study. *Oral Surg. Oral Med. Oral Pathol.* **32**, 865–875 (1971).
15. L. Eriksson, P.-L. Westesson, Temporomandibular joint diskectomy. No positive effect of temporary silicone implant in a 5-year follow-up. *Oral Surg. Oral Med. Oral Pathol.* **74**, 259–272 (1992).
16. R. J. Hinton, Alterations in rat condylar cartilage following discectomy. *J. Dent. Res.* **71**, 1292–1297 (1992).
17. L. N. Estabrooks, C. E. Fairbanks, R. J. Collett, L. Miller, A retrospective evaluation of 301 TMJ Proplast-Teflon implants. *Oral Surg. Oral Med. Oral Pathol.* **70**, 381–386 (1990).
18. C. H. Henry, L. M. Wolford, Treatment outcomes for temporomandibular joint reconstruction after Proplast-Teflon implant failure. *J. Oral. Maxillofac. Surg.* **51**, 352–358; discussion 359–360 (1993).
19. M. K. Murphy, B. Arzi, S. M. Prouty, J. C. Hu, K. A. Athanasiou, Neocartilage integration in temporomandibular joint discs: Physical and enzymatic methods. *J. R. Soc. Interface* **12**, 20141075 (2015).
20. K. Mäenpää, V. Ellä, J. Mauno, M. Kellomäki, R. Suuronen, T. Ylikomi, S. Miettinen, Use of adipose stem cells and polylactide discs for tissue engineering of the temporomandibular joint disc. *J. R. Soc. Interface* **7**, 177–188 (2010).
21. C. M. Juran, M. F. Dolwick, P. S. McFetridge, Engineered microporosity: Enhancing the early regenerative potential of decellularized temporomandibular joint discs. *Tissue Eng. Part A* **21**, 829–839 (2015).
22. K. Legemate, S. Tarafder, Y. Jun, C. H. Lee, Engineering human TMJ discs with protein-releasing 3D-printed scaffolds. *J. Dent. Res.* **95**, 800–807 (2016).
23. B. N. Brown, W. L. Chung, A. J. Almarza, M. D. Pavlick, S. N. Reppas, M. W. Ochs, A. J. Russell, S. F. Badylak, Inductive, scaffold-based, regenerative medicine approach to reconstruction of the temporomandibular joint disk. *J. Oral. Maxillofac. Surg.* **70**, 2656–2668 (2012).
24. C. K. Hagandora, J. Gao, Y. Wang, A. J. Almarza, Poly (glycerol sebacate): A novel scaffold material for temporomandibular joint disc engineering. *Tissue Eng. Part A* **19**, 729–737 (2013).
25. K. A. Athanasiou, R. Eswaramoorthy, P. Hadidi, J. C. Hu, Self-organization and the self-assembling process in tissue engineering. *Annu. Rev. Biomed. Eng.* **15**, 115–136 (2013).
26. J. C. Hu, K. A. Athanasiou, A self-assembling process in articular cartilage tissue engineering. *Tissue Eng.* **12**, 969–979 (2006).
27. D. J. Huey, J. C. Hu, K. A. Athanasiou, Unlike bone, cartilage regeneration remains elusive. *Science* **338**, 917–921 (2012).
28. R. F. MacBarb, A. L. Chen, J. C. Hu, K. A. Athanasiou, Engineering functional anisotropy in fibrocartilage neotissues. *Biomaterials* **34**, 9980–9989 (2013).
29. D. J. Drucker, P. L. Brubaker, Proglucagon gene expression is regulated by a cyclic AMP-dependent pathway in rat intestine. *Proc. Natl. Acad. Sci. U.S.A.* **86**, 3953–3957 (1989).
30. D. E. Anderson, K. A. Athanasiou, Passaged goat costal chondrocytes provide a feasible cell source for temporomandibular joint tissue engineering. *Ann. Biomed. Eng.* **36**, 1992–2001 (2008).
31. M. K. Murphy, T. E. Masters, J. C. Hu, K. A. Athanasiou, Engineering a fibrocartilage spectrum through modulation of aggregate redifferentiation. *Cell Transplant.* **24**, 235–245 (2015).
32. M. K. Murphy, D. J. Huey, A. J. Reimer, J. C. Hu, K. A. Athanasiou, Enhancing post-expansion chondrogenic potential of costochondral cells in self-assembled neocartilage. *PLOS ONE* **8**, e56983 (2013).
33. L. W. Huwe, W. E. Brown, J. C. Hu, K. A. Athanasiou, Characterization of costal cartilage and its suitability as a cell source for articular cartilage tissue engineering. *J. Tissue Eng. Regen. Med.* **12**, 1163–1176 (2018).
34. K. N. Kalpakci, V. P. Willard, M. E. Wong, K. A. Athanasiou, An interspecies comparison of the temporomandibular joint disc. *J. Dent. Res.* **90**, 193–198 (2011).
35. N. Vapniarsky, A. Aryaei, B. Arzi, D. C. Hatcher, J. C. Hu, K. A. Athanasiou, The Yucatan minipig temporomandibular joint disc structure–function relationships support its suitability for human comparative studies. *Tissue Eng. Part C Methods* **23**, 700–709 (2017).
36. L. W. Huwe, G. K. Sullan, J. C. Hu, K. A. Athanasiou, Using costal chondrocytes to engineer articular cartilage with applications of passive axial compression and bioactive stimuli. *Tissue Eng. Part A* **24**, 516–526 (2018).
37. E. A. Makris, D. J. Responte, N. K. Paschos, J. C. Hu, K. A. Athanasiou, Developing functional musculoskeletal tissues through hypoxia and lysyl oxidase-induced collagen cross-linking. *Proc. Natl. Acad. Sci. U.S.A.* **111**, E4832–E4841 (2014).
38. E. A. Makris, R. F. MacBarb, N. K. Paschos, J. C. Hu, K. A. Athanasiou, Combined use of chondroitinase-ABC, TGF-β1, and collagen crosslinking agent lysyl oxidase to engineer functional neotissues for fibrocartilage repair. *Biomaterials* **35**, 6787–6796 (2014).
39. D. J. Responte, B. Arzi, R. M. Natoli, J. C. Hu, K. A. Athanasiou, Mechanisms underlying the synergistic enhancement of self-assembled neocartilage treated with chondroitinase-ABC and TGF-β1. *Biomaterials* **33**, 3187–3194 (2012).
40. D. Xiao, J. Hu, K. Chen, C. Man, S. Zhu, Protection of articular cartilage by intra-articular injection of NEL-like molecule 1 in temporomandibular joint osteoarthritis. *J. Craniofac. Surg.* **23**, e55–e58 (2012).
41. B. Ying, K. Chen, J. Hu, C. Man, G. Feng, B. Zhang, S. Zhu, Effect of different doses of transforming growth factor-β_1 on cartilage and subchondral bone in osteoarthritic temporomandibular joints. *Br. J. Oral Maxillofac. Surg.* **51**, 241–246 (2013).
42. K. P. H. Pritzker, S. Gay, S. A. Jimenez, K. Ostergaard, J.-P. Pelletier, P. A. Revell, D. Salter, W. B. van den Berg, Osteoarthritis cartilage histopathology: Grading and staging. *Osteoarthritis Cartilage* **14**, 13–29 (2006).
43. X.-W. Liu, J. Hu, C. Man, B. Zhang, Y.-Q. Ma, S.-S. Zhu, Insulin-like growth factor-1 suspended in hyaluronan improves cartilage and subchondral cancellous bone repair in osteoarthritis of temporomandibular joint. *Int. J. Oral Maxillofac. Surg.* **40**, 184–190 (2011).

44. B. Zhang, J. Hu, C. Man, S. Zhu, Effect of intra-articular administration of interleukin 1 receptor antagonist on cartilage repair in temporomandibular joint. *J. Craniofac. Surg.* **22**, 711–714 (2011).
45. K. Chen, C. Man, B. Zhang, J. Hu, S.-S. Zhu, Effect of in vitro chondrogenic differentiation of autologous mesenchymal stem cells on cartilage and subchondral cancellous bone repair in osteoarthritis of temporomandibular joint. *Int. J. Oral Maxillofac. Surg.* **42**, 240–248 (2013).
46. E. Helmy, R. Bays, M. Sharawy, Osteoarthrosis of the temporomandibular joint following experimental disc perforation in *Macaca fascicularis*. *J. Oral. Maxillofac. Surg.* **46**, 979–990 (1988).
47. T. C. Lang, M. L. Zimny, P. Vijayagopal, Experimental temporomandibular joint disc perforation in the rabbit: A gross morphologic, biochemical, and ultrastructural analysis. *J. Oral. Maxillofac. Surg.* **51**, 1115–1128 (1993).
48. M. Miloro, B. Henriksen, Discectomy as the primary surgical option for internal derangement of the temporomandibular joint. *J. Oral. Maxillofac. Surg.* **68**, 782–789 (2010).
49. S. B. Milam, Failed implants and multiple operations. *Oral Surg. Oral Med. Oral Pathol. Oral Radiol. Endod.* **83**, 156–162 (1997).
50. K. P. Schellhas, C. H. Wilkes, M. el Deeb, L. B. Lagrotteria, M. R. Omlie, Permanent Proplast temporomandibular joint implants: MR imaging of destructive complications. *AJR Am. J. Roentgenol.* **151**, 731–735 (1988).
51. G. Dimitroulis, A critical review of interpositional grafts following temporomandibular joint discectomy with an overview of the dermis-fat graft. *Int. J. Oral Maxillofac. Surg.* **40**, 561–568 (2011).
52. M. S. Shive, J. M. Anderson, Biodegradation and biocompatibility of PLA and PLGA microspheres. *Adv. Drug Deliv. Rev.* **28**, 5–24 (1997).
53. C. M. Juran, M. F. Dolwick, P. S. McFetridge, Shear mechanics of the TMJ disc: Relationship to common clinical observations. *J. Dent. Res.* **92**, 193–198 (2013).
54. G. D. DuRaine, B. Arzi, J. K. Lee, C. A. Lee, D. J. Responte, J. C. Hu, K. A. Athanasiou, Biomechanical evaluation of suture-holding properties of native and tissue-engineered articular cartilage. *Biomech. Model. Mechanobiol.* **14**, 73–81 (2015).
55. S. W. Herring, The dynamics of mastication in pigs. *Arch. Oral Biol.* **21**, 473–480 (1976).
56. K. D. Allen, K. Erickson, K. A. Athanasiou, The effects of protein-coated surfaces on passaged porcine TMJ disc cells. *Arch. Oral Biol.* **53**, 53–59 (2008).
57. K. D. Allen, K. A. Athanasiou, Effect of passage and topography on gene expression of temporomandibular joint disc cells. *Tissue Eng.* **13**, 101–110 (2007).
58. A. J. Almarza, K. A. Athanasiou, Effects of hydrostatic pressure on TMJ disc cells. *Tissue Eng.* **12**, 1285–1294 (2006).
59. D. E. Johns, M. E. Wong, K. A. Athanasiou, Clinically relevant cell sources for TMJ disc engineering. *J. Dent. Res.* **87**, 548–552 (2008).
60. A. Crupi, A. Costa, A. Tarnok, S. Melzer, L. Teodori, Inflammation in tissue engineering: The Janus between engraftment and rejection. *Eur. J. Immunol.* **45**, 3222–3236 (2015).
61. S. A. Eming, T. A. Wynn, P. Martin, Inflammation and metabolism in tissue repair and regeneration. *Science* **356**, 1026–1030 (2017).
62. R. F. MacBarb, N. K. Paschos, R. Abeug, E. A. Makris, J. C. Hu, K. A. Athanasiou, Passive strain-induced matrix synthesis and organization in shape-specific, cartilaginous neotissues. *Tissue Eng. Part A* **20**, 3290–3302 (2014).
63. D. D. Cissell, J. M. Link, J. C. Hu, K. A. Athanasiou, A modified hydroxyproline assay based on hydrochloric acid in Ehrlich's solution accurately measures tissue collagen content. *Tissue Eng. Part C Methods* **23**, 243–250 (2017).
64. F.L. Carson, *Histotechnology: A Self-instructional Text* (ASCP Press, 1997).
65. P. Mehra, L. M. Wolford, Use of the Mitek anchor in temporomandibular joint disc-repositioning surgery. *Proc. (Bayl. Univ. Med. Cent.)* **14**, 22–26 (2001).

Acknowledgments: We thank W. Ferrier, L. Talken, and S. C. Döring for help with the surgeries. We also thank University of California Davis Campus Veterinary Services for help with animal care. We acknowledge C. Toupadakis for help with the artwork. M.K.H.'s work was partially supported while serving at the NSF. Any opinion, findings, and conclusions or recommendations expressed in this material are those of the authors and do not necessarily reflect the views of the NSF. **Funding:** This study was supported by NIH grant R01DE015038 (K.A.A.). **Author contributions:** N.V. and L.W.H. designed and carried out the study, acquired and interpreted the data, and prepared the manuscript. B.A., M.E.W., and J.W.W. contributed to the study design, performed the surgeries, and critically reviewed the manuscript. M.K.H. contributed to the study design, data acquisition, and interpretation of the data and critically reviewed the manuscript. D.C.H. contributed to the study design and acquired and interpreted the data. J.C.H. and K.A.A. designed the study, interpreted the data, critically reviewed the manuscript and its revisions, and gave final approval. **Competing interests:** The authors declare that they have no competing interests. **Data and materials availability:** All data are in the paper and Supplementary Materials.

Submitted 10 October 2017
Accepted 25 May 2018
Published 20 June 2018
10.1126/scitranslmed.aaq1802

Citation: N. Vapniarsky, L. W. Huwe, B. Arzi, M. K. Houghton, M. E. Wong, J. W. Wilson, D. C. Hatcher, J. C. Hu, K. A. Athanasiou, Tissue engineering toward temporomandibular joint disc regeneration. *Sci. Transl. Med.* **10**, eaaq1802 (2018).

Science Translational Medicine

Tissue engineering toward temporomandibular joint disc regeneration

Natalia Vapniarsky, Le W. Huwe, Boaz Arzi, Meghan K. Houghton, Mark E. Wong, James W. Wilson, David C. Hatcher, Jerry C. Hu and Kyriacos A. Athanasiou

Sci Transl Med **10**, eaaq1802.
DOI: 10.1126/scitranslmed.aaq1802

Disjointed no more

Temporomandibular joint (TMJ) dysfunction causes pain and limits movement of the jaw joint. Thinning of the TMJ disc, a fibrocartilage structure that allows for smooth joint movement, is an early sign of TMJ dysfunction. To help prevent joint degeneration, Vapniarsky *et al*. implanted engineered discs derived from rib cartilage cells into a minipig model of TMJ disc thinning. The implants had biomechanical and biochemical properties similar to native discs and improved closure of disc defects, reduced osteoarthritis scores, and reduced degenerative changes in the jaw joint. This scaffold-free approach to tissue engineering disc implants could help advance development of regenerative therapies for TMJ dysfunction.